Lawrence Berkeley Laboratory
UNIVERSITY OF CALIFORNIA

Materials & Molecular Research Division

HYDROGEN CHEMISORPTION ON Pt SINGLE
CRYSTAL SURFACES IN ACIDIC SOLUTIONS

Philip N. Ross, Jr.

April 1980

DISCLAIMER

This document was prepared as an account of work sponsored by the United States Government. While this document is believed to contain correct information, neither the United States Government nor any agency thereof, nor the Regents of the University of California, nor any of their employees, makes any warranty, express or implied, or assumes any legal responsibility for the accuracy, completeness, or usefulness of any information, apparatus, product, or process disclosed, or represents that its use would not infringe privately owned rights. Reference herein to any specific commercial product, process, or service by its trade name, trademark, manufacturer, or otherwise, does not necessarily constitute or imply its endorsement, recommendation, or favoring by the United States Government or any agency thereof, or the Regents of the University of California. The views and opinions of authors expressed herein do not necessarily state or reflect those of the United States Government or any agency thereof or the Regents of the University of California.

HYDROGEN CHEMISORPTION ON Pt SINGLE CRYSTAL SURFACES

IN ACIDIC SOLUTIONS

Philip N. Ross, Jr.
Lawrence Berkeley Laboratory
University of California
Berkeley, California 94720 (U.S.A.)

ABSTRACT

Hydrogen chemisorption from dilute acidic solution onto Pt single crystal surfaces was examined using an electrochemical cell directly coupled to LEED/Auger analytical system. No pre-anodization was used prior to observing hydrogen adsorption by cyclic voltammetry so that clean surfaces having the ordered structures indicated by LEED were studied. The problem of contributions from non-ordered parts of the electrode like support wires and edges was solved by using a gold evaporation masking technique. The specific contribution of atomic imperfections to the voltammetry curve was deduced from the ordered and countable imperfections occurring on high Miller index single crystal surfaces that have a stepped structure. The H-Pt bond energy was found to be structure sensitive, and sensitive both to local site geometry and long range order in the surface. The bond strength was found to vary systematically: n(111)x(100) > (100) > n(111)x(111) > (110) > (111). Distinct states for hydrogen at steps versus hydrogen on terraces could be distinguished. The (110) surface is shown to be a (111) vicinal, probably the [3(111) x 2(111)] microfacetted surface. The zero coverage heat of adsorption on the well-ordered (111) surface (48 kJ/mol) in solutions is the same as the value reported by Ertl and co-workers for adsorption on a (111) surface in vacuum. Adsorption isotherms for hydrogen on the (111) and (100) surfaces is adequately fit by the classical model for immobile adsorption at single sites with nearest neighbor repulsive interaction.

1. INTRODUCTION

In recent years a number of research groups have attempted to combine the contemporary methods of surface analysis with the traditional methods of electrochemistry, such as cyclic voltammetry, to obtain a definitive relation between electrode structure and the adsorption energy of intermediates. Three different research groups [1-3] have recently studied hydrogen adsorption on low index single crystal surfaces of Pt using Auger electron spectroscopy (AES) to monitor surface purity and low energy electron diffraction (LEED) to observe surface structure. The experimental procedures used in these studies differed, however, particularly in the manner in which the sample was transferred to the solution from the ultra-high vacuum system, and in the degree of pre-polarization applied prior to observation of hydrogen adsorption. Both the Yeager group [1] and the Hubbard group [2] incorporated the electrochemical cell into an ultra-high vacuum envelope which was back-filled with inert gas and electrolyte added from outside the vacuum system. In previous work by the author [3], the crystals were transferred via a vacuum line to a purged glove box containing a conventional electrochemical cell. The advantage of the glove box method is that the crystal could be mounted in a special holder that ensured metal-electrolyte contact only in the center of the crystal. In

the former systems, there was less control of the metal-liquid contact area, with support wires[2] and crystal edges[1] probably contributing to the total contacted area. The disadvantage of the glove box method was that contamination of the surface occurred upon transfer to the electrolyte, necessitating pre-polarization of the single crystal electrode to produce a clean surface. Post-test LEED analysis of the single crystal surfaces showed definitively that the pre-polarization above 1.0V* necessary to clean the electrode surface resulted in some restructuring. The volt-ammograms reported in[2] and[3] were, however, in reasonably good agreement, as were the adsorption energies for hydrogen on (111) and (100) surfaces. The results of the Yeager group[1] were somewhat different, particularly for the (111) surface where they reported very low coverage by hydrogen ($\sim$7 $\mu C/cm^2$), and they suggested a true difference may exist between adsorption at an annealed (111) surface that had never been pre-polarized above 1.0V and one which had, since their electrodes were not pre-polarized above 0.4V. The Yeager group also reported problems with wetting of the single crystal electrodes, which may account in part for the very low hydrogen charge per unit geometric area. However, the problem of pre-polarization must be regarded as unresolved, particularly with regard to the (111) surface.

The experimental problem of ex situ preparation of Pt electrodes for hydrogen electrosorption without anodic-cathodic pre-polarization has received attention in work with polycrystalline electrodes[4,5].

---

*All potentials refer to that against a reversible hydrogen electrode (10^2 kPa H_2) in the same electrolyte.

Clavilier and Chauvineau[4] have shown that argon sputter clean-
ing, even with intermediate air exposure, produced a voltammogram
without pre-polarization close to that suggested for "clean" poly-
crystalline Pt[6]. Thermal oxidation in the gas-phase with thermal
annealing in ultra-high vacuum also produced high coverages by
hydrogen without pre-polarization[5]. Multiple peaks observed for
hydrogen adsorption-desorption on Pt electrodes are, therefore,
associated with adsorption on clean, annealed Pt surfaces, and are
not restricted to non-equilibrium, defect surfaces produced by re-
peated anodic-cathodic pre-treatment.

If the multiple peaks in hydrogen electrosorption arise due princi-
pally to structure sensitivity, as the results of all the recent
single-crystal studies have suggested, then each peak for the
annealed polycrystalline surface should be related directly to a
peak observed on one of the low index faces. Several research
groups[1-3,7] have assigned the major "strong" hydrogen peaks to
adsorption at surface regions of (100) symmetry, and at least two
groups[1,3] assign the major "weak" hydrogen peak to adsorption
at regions of (111) symmetry. Kolb and co-workers[7] disagree
with the latter assignment and suggest the "weak" peak on poly-
crystalline Pt is associated with adsorption at (110) regions.
They suggest that reflection high energy electron diffraction
(RHEED) analysis of the (111) single crystal surface revealed
that twenty cycles to 1.3V restructured the (111) surface into
principally (110) facets. The peak maximum for hydrogen on their
(111) crystal was reported to be at about the same potential as
for the (110) crystal, but the peak shape was much broader and the

coverage lower. Upon potential cycling to 1.3V, they found the peak shape narrowed and the coverage increased and with fifteen cycles the voltammogram looked similar to that for the (110) crystal, consistent with the reconstruction indicated by their RHEED analysis of the cycled surface. These workers have therefore assigned the "weak" hydrogen peak on polycrystalline Pt to surface regions of (110) symmetry.

Fundamental differences in interpretation of the voltammetry curves for hydrogen on the low index single crystal surfaces of Pt have recently arisen. Conway[8] has emphasized that in all of the previous single-crystal studies, multiple peaks were observed for hydrogen electrosorption on each of the low index faces, and that these multiplicities may be evidence of "induced" heterogeneity in the adsorption-desorption process at a structurally homogeneous electrode surface. Even in the absence of anion specific adsorption[9,10], we have argued that the minor peaks can arise from intrinsic heterogeneity in the single crystal electrode, in the form of edges of the crystal, supporting wires, or imperfections on the crystal face itself. Since imperfections are introduced into the surface by potential cycling through the oxide formation region[3], it is imperative that hydrogen adsorption be observed on a clean surface with nearly perfect long range order without pre-anodization of the electrode in order to determine whether multiple adsorption states exist even on homogeneous surfaces.

In the present work we reexamined hydrogen electrosorption on the three low index faces of Pt, (111), (100) and (110), using an improved sample transfer system that preserved ultra-high vacuum conditions prior to contact of the electrode surface with the electrolyte. No pre-anodization was used prior to observing hydrogen adsorption by cyclic voltammetry, so that clean, nearly perfectly ordered surfaces were studied. The problem of contributions from non-ordered portions of the electrode like support wires and edges was solved using an evaporated gold film masking technique. In addition, the specific contribution of imperfections to the hydrogen electrosorption peaks was deduced by introducing ordered and countable imperfections by the use of high Miller index single crystal surfaces that have a stepped structure. Cyclic voltammetry of the stepped surface denoted [3(111)x(100)] in the notation of Lang et.al.[11] was reported in previous work, and we report here results for [4(111)x(111)], [4(111)x(100)] and [6(111)x(111)], [6(111)x(100)]. We also show that the (110) surface is actually a (111) vicinal surface, and that the (2 x 1) reconstructed surface, which is a relatively stable surface configuration, and appears to be the low energy surface for the solid/liquid interface, is probably the [3(111)x2(111)] microfacetted surface. The objective of this reexamination was to eliminate to the greatest possible extent the ambiguities arising in the interpretation of hydrogen electrosorption due to the use of less than perfect surface structures and to resolve the problem of hydrogen on the (111) Pt surface.

2. EXPERIMENTAL

The LEED-AES electrochemistry system was similar to that used in the previous work[3], but the electrochemical cell and transfer system were modified to provide a clean ultra-high vacuum environment up to the instant of contact of the single crystal with the electrolyte. The new electrochemical cell is shown schematically in Figure 1. The single crystals were spot-welded to gold wires and suspended from a stainless steel block. The block was transferred from the manipulator in the LEED-AES bell-jar to the electrochemical cell by means of two polished stainless steel rods; vacuum sealing of the rods was accomplished using Viton O-rings radially compressed. The working electrode compartment, and the high-vacuum parts of the system, were isolated from the electrolyte reservoir and reference electrode via a glass-break. The transfer system and working electrode compartment were differentially pumped to about 1.3×10^{-6} Pa (1×10^{-8} torr) after a bakeout at 423K. In the typical experiment, a new single-crystal was mounted on the transfer block and attached to the vertical motion transfer rod with the electrochemical cell detached. The transfer block was transferred to the horizontal motion rod, the electrochemical cell attached to the system, and the entire transfer system pumped out to 2×10^{-6} Pa. The single crystal was then transferred to the ultra-high vacuum system, where it was cleaned by simultaneous argon ion bombardment and electron beam heating to 973K. Depending on the crystal, this treatment sometimes required several hours before analysis by Auger electron spectroscopy indicated no sign of any detectable surface impurities. Typical impurities removed by hot ion bombardment were Ca, P, C and Si. The Auger spectrometer

system also had sample imaging capability (Varian Model 981-2757
Scanning Sample Positioner) so that the entire surface of the crys-
tal was analyzed for impurities. The structure of the surface was
then determined using LEED. After structure analysis was performed,
the crystal was transferred into the working electrode compartment
and the electrochemical system was isolated from the LEED-AES
system by closure of the straight-thru valve. The working elec-
trode compartment was then backfilled with Research Grade argon
(Airco, 5 N purity) to near ambient pressure, and the electrolyte
introduced by breaking the glass seal.

Triangular sweep cyclic voltammetry was carried out using a
Princeton Applied Research (Model 173) Potentiostat, an x-y recor-
der (Hewlett-Packard Model 7044A), and a sweep generator (Wavetek).
The reference electrode was a reversible hydrogen electrode, con-
sisting of a Pt wire mesh from which hydrogen was evolved periodi-
cally to maintain ca. 10^2 kPa hydrogen pressure in the reference.
The electrolytes were 0.5M H_2SO_4 and 0.05 $HClO_4$ prepared by dilu-
tion of concentrated acid (Baker, Ultrex grade) with water purified
by the method of Conway et.al.[12]. The electrolyte was pretreated
in the reservoir by anodic-cathodic potential cycling using Pt
foil electrodes (detail 7 in Figure 1) until the voltammogram was
representative of polycrystalline Pt in clean dilute $HClO_4$[10].
To conduct post-test LEED analysis of the single-crystal electrode,
the crystal was lifted from the electrolyte, the gate valve
(detail 4 in Figure 1) closed, and the transfer chamber ion pumped
to about 3 x 10^{-5} Pa prior to transfer to the LEED-AES chamber.

High purity single crystal rods of orientation (111), (100) and
(110) were obtained from MRC. The (111) and (100) rods were 0.95
cm diameter and the (110) rod was 0.64 cm. The low index rods were
spark cut into 1 mm slices after mounting and alignment using the
von Laue x-ray technique. The high Miller index crystals were pre-
pared by cutting the (111) and (100) rods at appropriate angles to
the [111] and [100] crystallographic axes after orientation on the
x-ray goniometer. The orientations of crystals used in this work
are shown in the stereographic projection in Figure 2. The crys-
tals were polished using standard metallographic techniques with
the final step a polish with 0.05 μm alumina powder. Before use,
the crystals were heat treated in a vacuum induction furnace for
12 hours at 1573K and dipped briefly in hot aqua regia to remove
impurities that accumulated at the surface during heat treatment.

Since the cell configuration employed here required complete sub-
mersion of the crystal, regions of the crystal that are not well-
ordered are contacted by electrolyte and thus contribute to the
voltammogram, e.g. the edge. Typically the geometric area of
edges on these crystals was 20% of the area of the polished faces,
and the effective area even greater because of roughness. The con-
tribution of the crystal edges to the voltammogram was measured
directly by a gold masking technique. After obtaining the voltam-
mogram for the complete crystal, gold was evaporated onto the
polished faces so that just the edges and near-edge region of the
Pt crystal were exposed to electrolyte. The voltammogram for these
disordered regions was obtained following the same procedure as
used for the crystal without the gold mask. To facilitate data

manipulation the voltammograms were digitized and recorded in a multi-channel analyzer (Tracor-Northern NS 575A).

3. RESULTS

3.1 Voltammetry of the Well-ordered Low Index Surfaces

Since the majority of Pt cyclic voltammetry has been done in H_2SO_4, we considered it appropriate to include some results on both polycrystalline Pt foils and low index single crystals in this electrolyte for comparison with other work. Figure 3 shows the voltammogram for a polycrystalline foil cleaned by ion bombardment and thermally annealed (1073K) and contacted with the electrolyte potentiostated at 0.4V. The first sweep was cathodic after about a 30s hold. Even on the first anodic sweep from 0.05V, where the electrode has never been to oxide formation potentials, four hydrogen peaks are resolved and only one sweep to 1.5V to remove impurities adsorbed primarily during the hold at 0.4V is needed to establish a voltammogram characteristic of a Pt foil in 0.5M H_2SO_4[6]. That the impurities came from the electrolyte was determined by repeating the potential hold at 0.4V after the 4th 0.05-1.5V cycle and observing essentially the first voltammogram. The glass walls of the working electrode compartment were probably the source of these impurities. This is clearly a minor problem as at least qualitative comparison can be made from the first sweep and quantitative data can be obtained after a single sweep through oxide formation. As we will show by post-test LEED analysis of the surface, this single sweep produced an immeasurably small perturbation to the surface structure. The results for the (111) and (100) crystal surfaces are

are shown in Figures 4 and 5. Contrary to the claims made
by the Yeager group[1], hydrogen is underpotentially deposi-
ted on a clean, well-ordered Pt (111) surface without any
anodic pre-polarization. The coverage was at least 0.5 based
on the geometric area of the electrode using 240 $\mu c/cm^2$ as
the total charge for unit coverage. For (111) Pt, hydrogen
adsorption-desorption produced primarily one peak at 0.10V
in 0.5M H_2SO_4 with some structure at higher potentials that,
as we will show subsequently, can be attributed to processes
at disordered regions of the single-crystal electrode.
Figure 5 gives the voltammogram for the (100) Pt crystal re-
corded as the second sweep from the 0.4V start, and compares
the result with the second sweep for the (111) Pt crystal.
For (100) Pt, hydrogen adsorption-desorption produced primarily
one peak at 0.26V with some additional structure at both higher
and lower potentials that can be attributed to processes at
disordered regions. It is interesting to note in Figure 5 the
dramatic difference in the oxide formation-reduction waves on
these two differently ordered surfaces, the process being much
more reversible on (100) Pt than on (111) Pt.

It is now well known[9,10] that a quantitative study of the
hydrogen electrosorption process cannot be made in an electro-
lyte like 0.5M H_2SO_4 because of close coupling of specific
anion adsorption with hydrogen electrosorption. Thus, all
quantitative studies should be done in either very dilute
$HClO_4$ or dilute HF. We choose 0.05M $HClO_4$ in order to use a
glass cell and to simplify the engineering of the apparatus.

Figures 6 and 7 show the hydrogen region of the voltammo-
gram for (111) and (100) Pt, respectively, for the second
sweep from the 0.4V start. After gold was vacuum evaporated
onto the faces of the crystals, the experiment was repeated
with the results shown as the dotted lines. These curves
represent underpotential hydrogen on the unmasked portion of
the electrodes, e.g. the crystal edges and support wires,
and of course the equilibrium hydrogen evolution-dissolution
process on the total surface. The difference curves (dashed)
therefore represent underpotential hydrogen on those parts
of the electrodes covered by the gold evaporant, which LEED
analysis has shown to be the well-ordered surface. For (111)
Pt, the result was a nearly symmetric single peak, whose inte-
grated area indicates a coverage by hydrogen of at least 0.5
of a monolayer (Figure 8) based on the geometric area under
the gold mask. For (100) Pt, the result was an asymmetric
single peak with an integral area indicating virtual satura-
tion of the surface by hydrogen at the equilibrium potential
(Figure 9).

3.2 Isotherms of Hydrogen on (111) and (100) Surfaces

For the sweep rates employed here the hydrogen adsorption-
desorption processes are at quasi-equilibrium, and adsorp-
tion isotherms may be obtained directly by integration of the
voltammetry curve. Then

$$i = \frac{dq}{dt} = vC_{dl} + vQ\frac{d\theta}{dU} \tag{1}$$

where v is sweep rate, Q the charge for forming a monolayer,
C_{dl} the double-layer capacity, $Qd\theta/dU$ the adsorption pseudo-

capacity, and U the electrode potential. Then

$$\theta = \int \frac{(i - vC_{dl})}{vQ} \, dU \qquad (2)$$

where i is the cathodic (adsorption) current. Since the voltam-
metry curves were digitized and stored in the NS-575 signal
averages, the double layer corrections and integrations were
carried out electronically and the resulting θ-U curve plotted.
The voltammetry curves corrected for adsorption at the edges
were used to generate the isotherms. The charge for forming
a monolayer was calculated from the geometric area of the two
faces of the crystals. Finally, the θ-log P_{H_2} relation is ob-
tained from the Nernst equation relating the electrode (under)
potential to the thermodynamic activity of gaseous hydrogen

$$U = -2.3\frac{RT}{2F} \log a_{H_2} = -2.3\frac{RT}{2F} \log P_{H_2} \qquad (3)$$

To help in the interpretation of the asymmetry in the adsorp-
tion peaks for the (111) and (100) surfaces, isotherms were
obtained at variable temperature (278-323K) and the isosteric
heats of adsorption calculated using the procedure of Boeld
and Breiter[13]. The results are given in Figure 10 and the
variation in the heat of adsorption with coverage shows that
the asymmetry does not arise due to unresolved peaks but is
caused by interaction between adsorbed hydrogens on the sur-
face. This point will be discussed in detail later in the
paper.

3.3   Voltammetry of Stepped Surfaces

The results for the (110) single crystal have been grouped with

the results for the (111) vicinal stepped surfaces for the
purposes of presentation and discussion. LEED analysis of
the clean annealed (110) crystal in vacuo indicated the sur-
face was reconstructed, as evidenced by the presence of half-
order spots in the [001] direction that produced a (2 x 1)
diffraction pattern. This (2 x 1) reconstructed (110) sur-
face has been observed by numerous groups[14], including
Yeager et.al.[1], and Ducros and Merrill have proposed a
"sawtooth" structure (see Figure 11) consisting of tilted
(111) microfacets for the (110)-(2 x 1) surface. In the
stepped surface notation, this surface structure would be
$[3(111)x2(111)]$. The same structure has been proposed for
the (110)-(2 x 1) surfaces of Ir and Au, and is also suppor-
ted by the ion backscattering results of Davies et.al.[15]
that indicated the number of scattering centers at normal inci-
dence was twice that expected for a (110)-(1 x 1) surface.
The structure along the step of an $[n(111)x(111)]$ surface is
exactly the same as the structure in the "trough" of the
(110)-(2 x 1), as a comparison of Figures 10a. and 10b. makes
clear. The LEED patterns for the Miller index (221) and (775)
crystals in vacuo were exactly those expected for the stepped
surface geometries, $[4(111)x(111)]$ and $[7(111)x(111)]$, respec-
tively, using the kinematic model of Ellis and Schwoebel[3,16].
It was expected, therefore, that a comparison of crystals (111),
(775), (221) and (110) would reveal the effect of adsorption at
the four-fold sites (designated C_{110}^4) that exist at the steps
in the $[n(111)x(111)]$ surfaces and at the "trough" of the

(110)-(2 x 1) surface. For this series of experiments, the
edges of the crystals were masked by vacuum evaporation of
a gold film. The results shown in Figure 12 bore out these
expectations to a remarkable degree. The ratio of four-fold
step sites (C_{110}^4) to the three-fold hollow sites (C_{111}^3) on the
terraces varied in this series from 0, to 1:6, to 1:3 and to
1:1, respectively. The (221) and (110) crystals showed a
clearly delineated second peak occurring at 0.225V and the
ratio of peak areas (after computer deconvolution) was about
the 1:3 and 1:1 expected if we assign the second peak to adsorp-
tion at the C_{110}^4 sites. The voltammogram for the (775) crystal
was essentially indistinguishable from the result for the (111)
crystal which had additional structure on the high potential
side of the main peak. This additional structure can reason-
ably be attributed to adsorption on parts of the crystal edge
not masked by the evaporated gold (this surface was very rough)
and on the regions of the crystal faces near the edge, which
were clearly imperfect when examined by scanning electron micro-
scopy. In repeating the experiment with three different (111)
crystals, the structure on the side of the main peak varied
noticeably, illustrating how difficult it is experimentally to
eliminate reproducibly the contributions due to imperfect
regions of the crystal. It was concluded that we coult not
make a quantitative distinction between hydrogen adsorption at
the (111) surface and at the [7(111)x(111)] surface in this
series of experiments. However, with the [4(111)x(111)] and
the (111)-(2 x 1) surfaces, the distinctions were clear owing
to the high concentration of the C_{110}^4 sites.

Just as the crystals produced by cutting a (111) rod at sequentially increasing angles toward the [110] pole revealed adsorption at sites having the (110) geometry, cutting the (111) rod at sequentially increasing angles towards the [100] pole revealed adsorption at sites characteristic of (100) geometries. The LEED patterns for the Miller index (755) and (533) crystals in vacuo had the split spot pattern expected for the stepped surface geometries [6(111)x(100)] and [4(111)x(100)]. The (211) crystal had the stepped structure [3(111)x(100)] and the cyclic voltammetry of this surface was discussed in detail in previous work[3] so we present it here only for comparison with the other vicinal surfaces. If we assume that adsorption at the steps occurs at the four-fold sites of (100) geometry (C_{100}^4) and at the terraces in the three-fold sites of (111) geometry (C_{111}^3), then the ratio of step sites to terrace sites on the crystals (111), (755), (533) and (211) would be 0, 1:6, 1:3, and 1:2 respectively. States associated with the steps are clearly delineated in the voltammograms of Figure 13, and the total charge associated with the steps was about that expected if only half the (111) sites are filled, as was the case for the ordered (111) crystal. However, unlike the (111) steps, two states of hydrogen are associated with adsorption at (100) steps, one state being more strongly bound at the (100) step than at the ordered surface of the same symmetry.

4. DISCUSSION

4.1 Comparison With Previous Work

The voltammetry curves for the polycrystalline foil (Fig. 3), and the (111) and (100) crystals (Figs. 4, 5) in 0.5M H_2SO_4, without anodic pre-treatment, are very similar to those reported by Hubbard et.al.[2]. The single peak for adsorption at the (111) surface is much sharper, and the coverage significantly higher (1.0 vs. 0.5) in the former work. Hubbard et.al.[2] apparently used some anodic pre-treatment and we postulate that the differences in the results arise from the anodic pre-treatment, since it has been observed[3,7] that even a few cycles of a (111) crystal through oxide formation-reduction causes both a narrowing of the voltammetry peak and an increase in charge under the peak. The voltammetry curve for the (100) crystal in 0.5M H_2SO_4 is nearly identical to that reported by both Hubbard et.al.[2] and Yamamoto et.al.[7] and there seems to be no controversy with regard to that surface. Yamamoto et.al. report a voltammetry curve for the (111) surface that is significantly broader (0.2V vs. 0.12V FWHM) and with slightly lower coverage (0.4 vs. 0.5) than we found here. This difference can be attributed directly to adsorption of impurities onto the single crystal surface during the atmospheric exposure in their experiments. We have repeated our experiment with the (111) crystal by back-filling the transfer chamber with air instead of ultra-pure argon; this produced a first sweep with a much broader

peak and lower coverage. Atmospheric contamination was ob-
served to have a more dramatic effect on the (111) single
crystal than any other single crystal surface. This should
not be too surprising, as this surface has the lowest heat
of adsorption and the largest adsorbate-adsorbate interac-
tion probability of any of the ordered surfaces.

It is difficult to make a quantitative comparison of our re-
sult for the (110) crystal with that of Yamamoto et.al. be-
cause of the reconstruction of this surface. RHEED, the
structure analysis used there, is not sensitive to recon-
struction of only the outermost layer of atoms (which is the
only atomic layer affected in the (2x1) reconstruction) so
that the structure of the surface of their (110) crystal was
not known. A comparison of the present result for the
(110)-(2x1) surface in 0.05M $HClO_4$ with their result for a
(110) crystal in 0.5M H_2SO_4 revealed significant differences.
However, even with possible differences in surface structure,
the principal difference between our result in 0.05M $HClO_4$
and their result in 0.5M H_2SO_4 can be attributed to the ad-
sorption of anions in sulfate solution. Figure 14 shows the
remarkable effect of HSO_4^- anions on the width of the voltam-
metry curve and the splitting of the two peaks for the
(110)-(2x1) surface. Addition of H_2SO_4 up to the 10^{-2}M
level further narrowed the curve to the point where the
high energy peak, attributable to adsorption in the (110)

trough, is barely distinguishable. The resulting curve in 0.05M $HClO_4$ + 0.01M H_2SO_4 is very similar to that reported by Yamamoto et.al.[7].

The isosteric heats of adsorption reported here for the (111) and (100) surfaces in acidic solution are not very different from those found by Will[29] if allowance is made for the fact that Will's single crystals were structurally heterogeneous. For (100), the initial heat of adsorption was 80 kJ/mol, which compares favorably with the present work. For (111), Will reported a heat of adsorption that was 59 kJ/mol at zero coverage and that dropped sharply at $\theta \simeq 0.6$ to 40 kJ/mol. Will's voltammetry curves, however, indicate that $1.0 < \theta < 0.6$ corresponds to adsorption at (100) vicinals, so that the transition at $\theta \simeq 0.6$ in the heat of adsorption curve probably corresponds to adsorption at (111) vicinals with Pt-H bond energy comparable to that found in the present work.

4.2   Structurally Homogeneous Surfaces

We consider now the problem of a possible multiplicity of states for hydrogen on a structurally homogeneous surface. The voltammetry curves shown in Figures 6 and 7 represent the nearest one can come in the present state of the art to observation of adsorption on a structurally homogeneous surface. Specific contributions from structurally imperfect regions of the crystals were accounted for quantitatively, and no prepolarization was used that might disturb the surface from the degree of perfection attained in vacuo. Quantitative analysis of the LEED patterns, after Park et.al.[30], indicated that the number of dislocations in the (111) and (100) crystal surfaces could not exceed one atom in every thirty atoms and produce the patterns observed. Thus, the marked asymmetry of the voltammetry curve for hydrogen on the structurally homogeneous (100) surface is due either to adsorption at sites on the surface of different symmetry, e.g. A-top, bridged or four-fold hollow sites, or due to a lateral interaction between adsorbed hydrogens. If there were adsorption at sites of distinctly different binding energy (corresponding to buried peaks), one would expect to see dips in the heat of adsorption vs. coverage curve corresponding to the progressive filling of sites of different bond energy. As Figure 10 shows, this was clearly not the case, although a multiplicity of states of nearly identical binding energy cannot be ruled out on the basis of this

argument. The essentially monotonic decrease in heat of adsorption with coverage and the asymmetry of the pseudocapacitance curve are consistent with adsorption on an energetically homogeneous surface.

Consider a non-ideal isotherm having the general form

$$\frac{\theta}{1-\theta} = P_{H_2}^{\frac{1}{2}} \exp\left[\Delta G_{ads}(\theta)/2RT\right] \tag{4}$$

where $\Delta G_{ads}(\theta)$ is the free energy change in the adsorption reaction

$$H_2 + 2M \rightleftharpoons 2M - H \tag{5}$$

which is a function of the extent of reaction, and θ is the coverage by adsorbed hydrogen. Non-ideal isotherms present a problem in defining a standard state. This problem has been carefully considered in the work of Conway et.al.[17] and we shall not pursue it further here. The free energy function $\Delta G_{ads}(\theta)$ can be calculated in a rigorous way from a number of models for dissociative adsorption. For the differential heats of adsorption we use the classic models presented by Roberts[18] for adsorption on identical sites with nearest neighbor interaction. For a system of uniform sites, the adsorption entropy for a diatomic molecule varies slowly with coverage for $\theta < 0.9$ and for the purposes of this analysis we will treat ΔS_{ads} as invariant. Then

$$\Delta G_{ads}(\theta) = -W(\theta) - T \Delta S_{ads} \tag{6}$$

where $W(\theta)$ is the differential heat of adsorption. If the
hydrogen adatoms are mobile at the temperature of adsorption,
then

$$W(\theta) = W_O - zV \left[1 - \frac{1-2\theta}{\{1-4(1-\rho)\theta(1-\theta)\}^{\frac{1}{2}}}\right] \qquad (7)$$

where ρ is the Boltzman factor $\exp(-V/RT)$, W_O is the initial
(zero coverage) heat of adsorption, and V is the pair-wise
interaction energy. For repulsive interaction, $V > 0$ and the
heat of adsorption decreases with coverage; for $|V| < RT$,
Taylor series expansion of (7) yields a linear change in the
heat of adsorption

$$W(\theta) = W_O - zV\theta \qquad (8)$$

Adsorption isotherms with a linear variation in adsorption
free energy have been used extensively for the modeling of
underpotential deposition[e.g. 19] and it is well known that
the linear function does not produce an asymmetric pseudocapa-
city curve. However, if the hydrogen adatoms are immobile,
the resulting isotherm produces an asymmetric pseudocapacity
curve and a heat of adsorption function which fits the observed
variation extremely well. For immobile adsorption,

$$W(\theta) = W_O - zV \left[\frac{(z-1)^2}{z} \theta \frac{(2z-\theta)}{(z-\theta)}\right] \qquad (9)$$

The best values of ΔG_{ads}^O, the free energy of adsorption at
zero coverage, and V were derived by curve fitting eq.(9) to
the isotherms for the (111), $z = 6$, and the (100), $z = 4$, sur-
faces simultaneously, then checking the resulting $W(\theta)$ function
against the experimentally observed variation. The best-fit

values of ΔG^o_{ads}, ΔS_{ads}, and V are given in Table 1, the calculated isotherms and the calculated W(θ) functions appear as the solid curves in Figures 6, 7 and 10, respectively. It is important to note that the derived values of ΔS_{ads} are very close $\left[\pm 12 \text{ J K}^{-1} \text{ mol}^{-1} \right]$ to the values expected for immobile adsorption of a diatomic molecule[20]. While the theoretical isotherms are not a perfect fit to the experimental curves, the asymmetry of the voltammetry curve for the (100) surface is predicted as well as the general form of the functional relation between isosteric heat of adsorption and coverage.

A comparison of the bond energies of adsorbed hydrogen on Pt single crystal surfaces immersed in an aqueous acidic medium with bond energies for single crystal surfaces in vacuum reveals some interesting trends. The initial (zero coverage) heats of adsorption for single crystals in vacuum are reported by McCabe and Schmidt[21] to be 73.2 kJ mol^{-1} for (111) and 102.4 kJ mol^{-1} for (100) with a pair-wise interaction energy of 13.2 kJ mol-pair^{-1}. Ertl and co-workers[22] reported much smaller values for hydrogen on (111), 41.2 kJ mol^{-1} and have shown that poorly annealed imperfect (111) crystals produced a high energy state with a heat of adsorption of 67 kJ mol^{-1}. Since McCabe and Schmidt did not have LEED optics in their system, it is possible they worked with imperfect surfaces, since their results for (111) are similar to the imperfect (111) surfaces of Ertl et.al. The bond energies found in this work for Pt (111) single crystals in aqueous solution are remarkably

close to those reported by the Ertl group for Pt (111) in
vacuum. If we assume the McCabe and Schmidt results for (100)
are on an imperfect crystal, with defects like the atomic
steps on n(111)x(100) surfaces, then the zero coverage heat
of adsorption we find here for hydrogen on n(111)x(100) sur-
faces in aqueous solution (98 kJ mol^{-1}) is nearly identical
to that in vacuum (102.4 kJ mol^{-1}). That the heat of adsorp-
tion of hydrogen on Pt in acid solution is close to that for Pt
in vacuum is not a new observation, as it was made perhaps
first by Breiter[23] and later by others[24]. Apparently the
Pt - H_2O specific interaction is very weak and H_2O molecules
are easily displaced from the surface with virtually no effect
on the Pt - H bond energy. Recent studies of water layers on
Pt (111) by thermal desorption, photoemission and vibration
spectroscopy[25] have confirmed the weak nature of the chemical
interaction of H_2O molecules with the Pt surface.

4.2   Adsorption at Periodic Imperfections

It was hoped that the problem of the minor peaks in the voltam-
metry of polycrystalline Pt electrodes in dilute $HClO_4$ or HF
would be resolved in a definitive way by the use of surfaces
with periodic atomic dislocations of precise number and struc-
ture. Unfortunately, this does not appear to be possible at
this time principally because the reconstruction of the (110)
single crystal surface makes direct relation to polycrystalline
surfaces a difficult matter. Certain assignments for adsorp-
tion at "defects" (high coordination sites) does appear possible,

however. Adsorption at n(111)x(100) steps results in the
most strongly bound (98 kJ mol^{-1}) state of hydrogen on Pt in
acidic solution but this state is not usually seen on poly-
crystalline electrodes, and, apparently, sites of this geometry
do not occur in significant concentrations on most elec-
trode surfaces. Adsorption at the (110)-(2 x 1) surface and
its vicinals, n(111)x(111), also indicated that hydrogen is
more strongly bound at the high coordination sites (C_{110}^{4})
found at the step than at sites on the low index terrace (C_{111}^{3}).
However, the structure sensitivity is much smaller in these
surfaces, as the heat of adsorption differs by only 15 kJ mol^{-1}
between the high and low coordination sites. In voltammograms
of polycrystalline Pt in non-adsorbing electrolytes (dilute
$HClO_4$ or HF), both from this laboratory[3] and from other
groups[10,26], there is a peak (denoted H_2 in Figure 15) loca-
ted 60-80 mV anodic of the principal "weak" hydrogen peak (H_1),
and we could reasonably associate this peak with adsorption at
the four-fold sites of the n(111)x(111) step geometry (C_{110}^{4}).
On none of the surfaces examined here was there the observation
of the much discussed[27] "third anodic peak" (H_3), usually
observed just to the cathodic side of the principal "strong"
hydrogen peak. Loo and Furtak[28] have shown this peak is not
an equilibrium state of hydrogen on Pt, but occurs only under
potentiodynamic conditions with cycling through oxide forma-
tion and reduction. The experimental conditions employed here
were designed to study only equilibrium states of hydrogen on
Pt and we would not, therefore, expect to see this state in
this study.

If a species is adsorbed at only one type of site on a structurally homogeneous surface, then the initial (zero-coverage) differential heat of adsorption represents the bond energy for sites of that geometry. The differential heat of adsorption at finite coverage will be less than the zero-coverage value due to repulsive interactions between adsorbates. The shape of the adsorption pseudocapacitance curve (and the isotherm) therefore depends on the symmetry at the adsorption site and the structural relation of sites of a given symmetry to one another. For example, adsorption at an ordered microdomain of sites will not produce the same isotherm as adsorption on the same sites in perfect long range order with one another, since the sites along the domain edge experience a different local environment. This exact effect is shown in a very precise way by the stepped surfaces. The terraces of stepped surfaces are micro-domains of the same symmetry separated by atomic dislocations of controlled structure. The comparison of n(111)x(111) and n(111)x(100) with (111) clearly demonstrated that the dislocations have two effects: (a) introduction of sites of different local symmetry and, thus, of different binding energy; (b) reduction of the interaction between hydrogen adsorbed within the ordered domain (the terrace). The change in adsorbate interaction causes a narrowing of the voltammetry curves and an increase in saturation coverage relative to the structurally perfect (111) surface. Because of these effects, only the voltammetry curves for stepped surfaces are likely to approximate adsorption at a

polycrystalline surface and be useful in relating various features in the voltammetry to specific structure.

A comparison of the voltammetry curves for the n(111)x(111) and n(111x(100) surfaces in Figures 12 & 13 with that characteristic of an annealed polycrystalline foil in Figure 15 (refer to ref. 3 for pre-treatment conditions) provide at least qualitative identification of the structure sensitive features in the curves. Assignment of each feature to a type of adsorption site can reasonably be made: H_1 with sites of (111) symmetry (C_{111}^3), H_2 with sites of the (110) "trough" symmetry (C_{110}^4), and H_4 with sites of the (100) symmetry (C_{100}^4). It is not possible, however, to further ascribe particular features in the curves to adsorption on micro-domains of certain short range order because of the complications of surface reconstruction, particularly in the case of the (110) surface. In this work we have studied the (2x1) reconstructed surface of a (110) single crystal which is easily formed in a vacuum and is stable in aqueous solution. Whether microdomains of (110) macroscopic orientation reconstruct to form this same surface is not known. Yamamoto et.al.[7] ascribe the "weak" hydrogen peak in 0.5M H_2SO_4 to adsorption on (110) domains. This assignment is certainly possible and consistent with the observations in the present work. However, other structures are possible, e.g. (111) domains connected by atomic dislocations of both (100) and (111) geometry, and a definitive analysis of voltammetry curves for polycrystalline electrodes

requires an independent determination of the structure, i.e.
one cannot determine structure of a specific Pt surface from
the shape of its voltammetry curve.

ACKNOWLEDGEMENTS

REFERENCES

1. E. Yeager, W. O'Grady, M. Woo and P. Hagans, J. Electrochem. Soc.,
    125, 348 (1978).

2. A. Hubbard, R. Ishiskawa and J. Kutakaru, J. Electroanal. Chem.,
    86, 271 (1978).

3. P. Ross, Jr., J. Electrochem. Soc., 126, 67 (1979).

4. J. Clavilier and J. Chauvineau, J. Electroanal. Chem., 100, 461 (1979).

5. V. Bagotzky, V. Lukyanychev, L. Frokina and N. Shumilova, J. Electro-
    anal. Chem., 98, 159 (1979).

6. H. Angerstein-Kozlowska, W. Sharp and B. Conway, in "Proceedings of the
    Symposium on Electrocatalysis", M. Breiter ed., The Electrochemical
    Society, Princeton, N.J. (1974), pp 94-114.

7. K. Yamamoto, D. Kolb, R. Koetz and G. Lempfuhl, J. Electroanal. Chem.,
    96, 233 (1979).

8. B. Conway and H. Angerstein-Kozlowska, Extended Abstracts, 155th Meet-
    ing of the Electrochemical Society, Boston, Mass., May 6-11, 1979,
    The Electrochemical Society Inc., pp 859-861.

9. P. Ross, Jr., J. Electroanal. Chem., 76, 139 (1977).

10. J. C. Huang, Ph.D. Thesis, Case Western Reserve University, 1976;
    J. Huang, W. O'Grady, and E. Yeager, J. Electrochem. Soc., 124, 1932 (1977).

11. B. Lang, R. Joyner, and G. Somorjai, Surf. Sci., 30, 440 (1972).

12. B. Conway, H. Angerstein-Kozlowska, W. Sharp and E. Criddle, Anal. Chem.,
    45, 1331 (1973).

13. W. Boeld and M. Breiter, Zeit. Elektrochem., 65, 897 (1960).

14. R. Ducros and R. Merrill, Surf. Sci., 55, 227 (1977); M. Salmeron and G. Somorjai, Lawrence Berkeley Laboratory Report, LBL-8464, 1979, to be published in Surface Science, 1980.

15. J. Davies, D. Jackson and P. Norten, Proc. 7th Int. Congr. and 3rd Int. Congr. Solid Surfaces (Vienna, 1977), p 2527.

16. W. Ellis and R. Schwoebel, Surf. Sci., 11, 82, (1968).

17. B. Conway, H. Angerstein-Kozlowska, and H. Dhar, Electrochim. Acta, 19, 455 (1974).

18. J. K. Roberts, "Some Problems in Adsorption", Cambridge University Press (1939), pp 21-41.

19. H. Angerstein-Kozlowska, J. Klinger and B. Conway, J. Electroanal. Chem., 75, 45 (1977).

20. A. Clark, "The Theory of Adsorption and Catalysis", Academic Press, (1970), pp 35-46.

21. R. McCabe and L. Schmidt, Proc. 7th Intern. Vac. Congr. and 3rd Intern. Conf. Solid Surfaces (Vienna, 1977), p 1201.

22. K. Christmann and G. Ertl, Surf. Sci., 60, 365 (1976); K. Christmann, G. Ertl and T. Pignet, Surf. Sci., 54, 365 (1976).

23. M. Breiter, "Electrochemical Processes in Fuel Cells", Springer-Verlag (New York), 1969, p 55.

24. P. Stonehart and P. N. Ross, Jr., Catal. Rev. - Sci. Eng., 12, 1 (1975); D. Ferrier, K. Kinoshita, J. McHardy and P. Stonehart, J. Electroanal. Chem., 61, 233 (1975).

25. G. Fisher and B. Sexton, General Motors Research Publication GMR-3108R, November 1979, submitted to Phys. Rev. Letters.

26. B. Conway, H. Angerstein-Kozlowska, and F. Ho, J. Vac. Sci. Technol., 14, 351 (1977).

27. K. Kinoshita, J. Lundquist and P. Stonehart, J. Catal., 31, 325 (1973) and references therein.

28. B. Loo and T. Furtak, to be published in Electrochim. Acta, 1980.

29. F. Will, J. Electrochem. Soc., 112, 451 (1965).

30. R. Park, J. Houston and D. Schreiner, Rev. Sci. Instr., 42, 60 (1971).

Table 1. Thermodynamic Functions[†] for the Adsorption of Hydrogen
          on Pt Single Crystal Surfaces.

Surface	ΔG_{ads}^{o} (kJ/mol)	ΔH_{ads}^{o} (kJ/mol)	ΔS_{ads}^{o} (J/mol-K)	V (kJ/mol-pair)
(111)	-30.1	-46.8	55.8	5.0
(100)	-65.2	-81.1	53.1	5.0

† zero coverage at 300K.

FIGURE CAPTIONS

Figure 1   - Schmatic of the electrochemical-surface analysis apparatus:
(1) O-ring feedthrus; (2) transfer rods; (3a and b) transfer
block with crystal suspended from wires; (4) gate valve;
(5) straight-thru valve; (6) reference electrode; (7) counter
electrodes; (8) glass-break and Luggin capillary.

Figure 2   - Stereographic triangle showing orientations of single crystal
surfaces studied in this work.

Figure 3   - Cyclic voltammetry of a clean, annealed polycrystalline Pt foil
in 0.5M H_2SO_4 following transfer from the LEED/Auger chamber.
50 mV/sec.

Figure 4   - Cyclic voltammetry of a (111) Pt single crystal in 0.5M H_2SO_4.
Potentiostated on immersion at 0.4V. 50 mV/sec.

Figure 5   - Cyclic voltammetry of a (100) Pt single crystal in 0.5M H_2SO_4
(——) compared to the (111) Pt crystal (----). 50 mV/sec.

Figure 6   - Voltammetry curve for hydrogen adsorption-desorption on Pt (111)
single crystal (——); specific contribution due to crystal
edge (...); curve for adsorption on the well-ordered (111)
face after correction for the edge effect. 0.05M $HClO_4$. 50 mV/sec.

Figure 7   - Voltammetry curves for hydrogen adsorption-desorption on Pt (100)
single crystal (——); specific contribution due to crystal
edge (...); curve for adsorption on the well-ordered (100) face
after correction for the edge effect. 0.05M $HClO_4$. 50 mV/sec.

Figure 8   - Isotherm for hydrogen on the well-ordered (111) Pt surface (0);
isotherms calculated from Langmuir model (---) and Roberts'
model for immobile adsorption with repulsive interaction (——).
300 K.

Figure 9   -   Isotherm for hydrogen on the well-ordered (100) Pt surface (O);
            isotherms calculated from Langmuir model (---) and Roberts'
            model for immobile adsorption with repulsive interaction (-----).
            300 K.

Figure 10 - Isosteric heats of adsorption of hydrogen on (111) and (100) sur-
            faces of Pt in dilute $HClO_4$ solution. Curves shown were calculated
   from Roberts' model for immobile adsorption with repulsive inter-
            action.

Figure 11 - Ball models of (a) the (100)-(1x1) unreconstructed surface (right)
            and the reconstructed (110)-(2x1) surface (left); (b) the
            $[4(111)x(111)]$ stepped surface. Small clear balls represent the
            four-fold adsorption sites denoted C_{110}^4 in the text.

Figure 12 - Voltammetry curves for hydrogen adsorption-desorption on
            n(111)x(111) stepped surfaces. 0.05M $HClO_4$. 50 mV/sec.

Figure 13 - Voltammetry curves for hydrogen adsorption-desorption on
            n(111)x(100) stepped surfaces. 0.05M $HClO_4$. 50 mV/sec.

Figure 14 - Effect of specific adsorption of HSO_4^- anion on the pseudocapacity
            curve for hydrogen on the (110)-(2x1) surface. 50 mV/sec.

Figure 15 - Voltammetry curves for hydrogen adsorption-desorption on a poly-
            crystalline Pt electrode (see ref. 3 for conditions). Multiple
            states of the adsorbed hydrogen are designated H_1 to H_4.
            0.05M $HClO_4$. 50 mV/sec.

to UHV chamber

5

to Ion pump

3a

to N₂ backfill manifold

3b

4

6

7

9

8

2

1
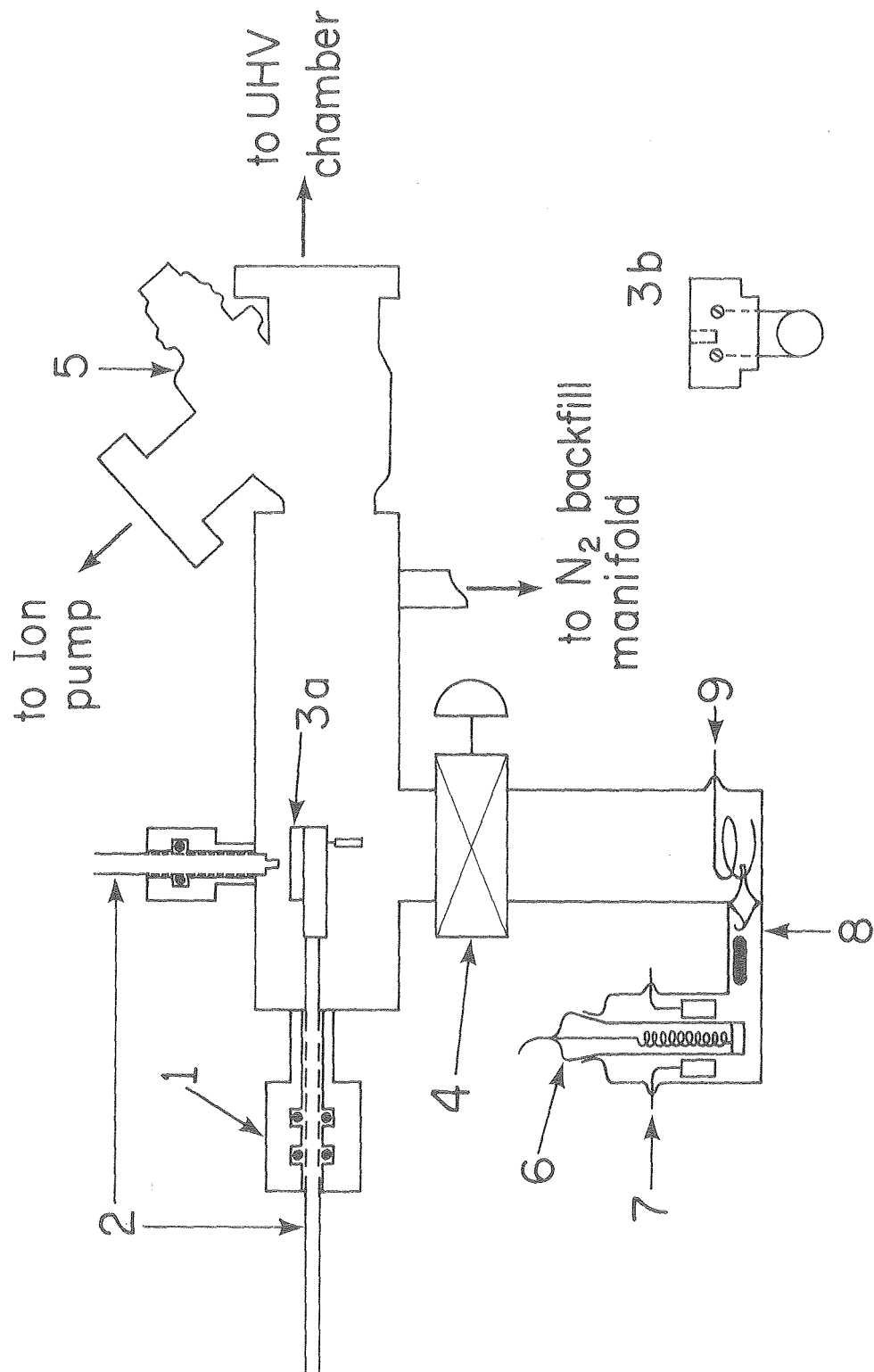
XBL 798-2475
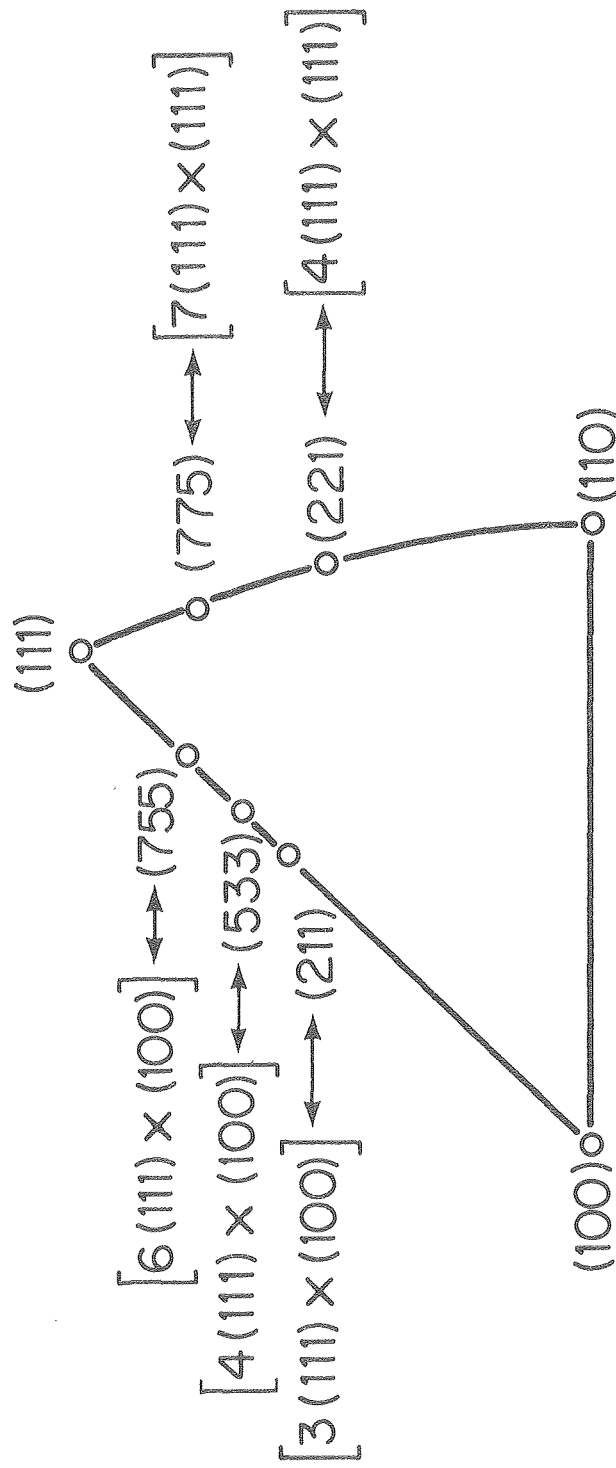
Fig. 1

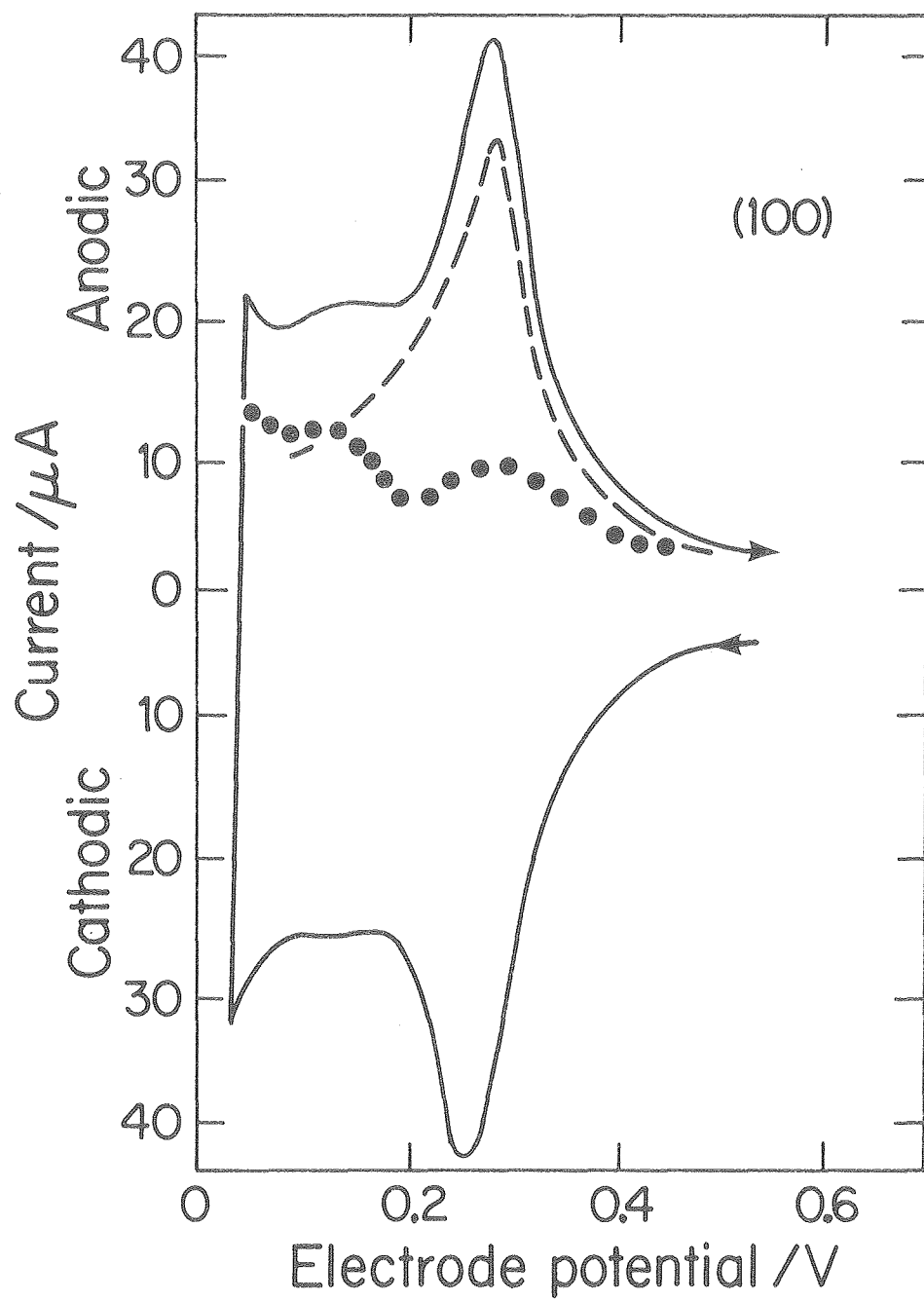Fig. 2
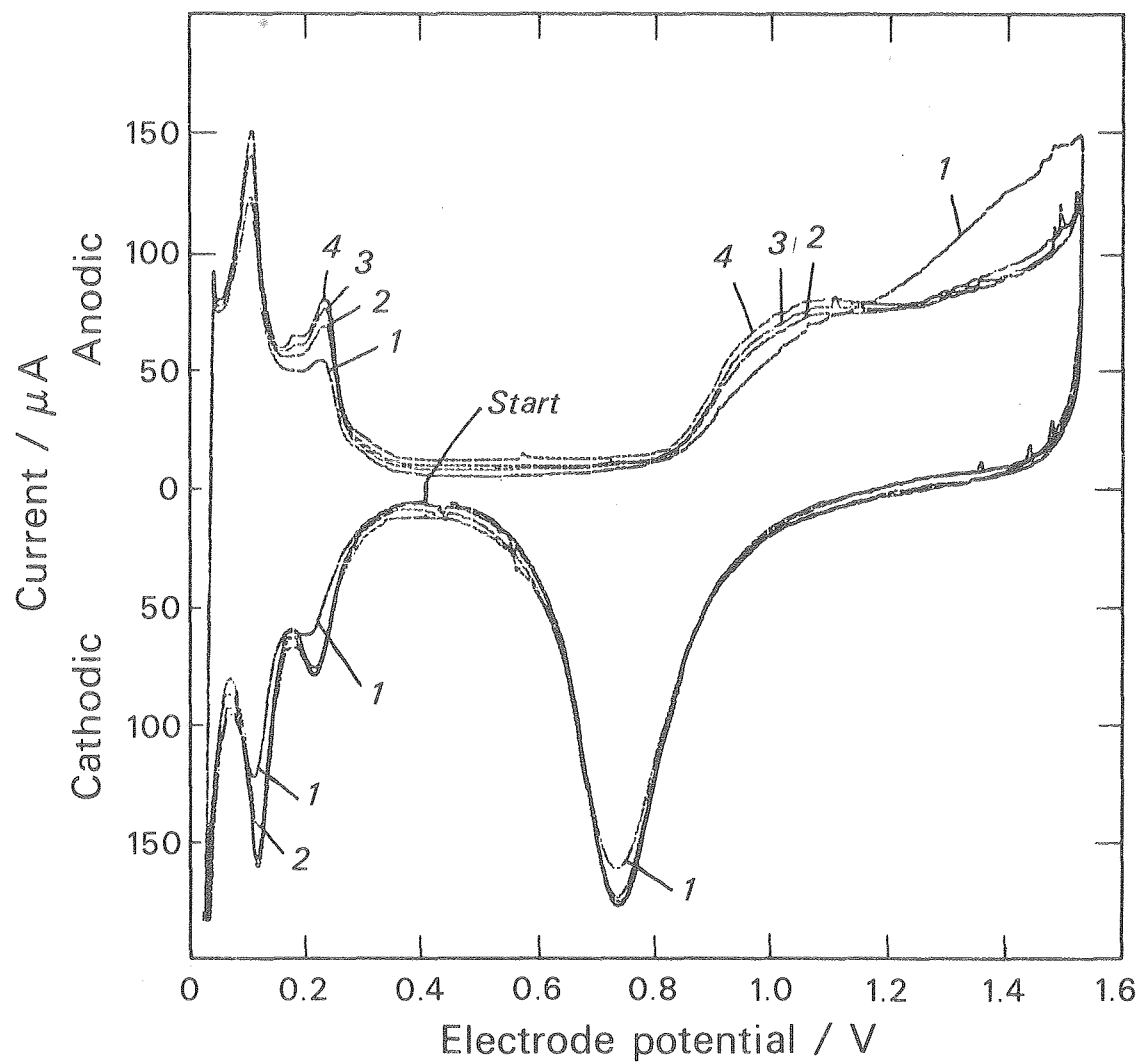
XBL 801-6

XBL 804-666

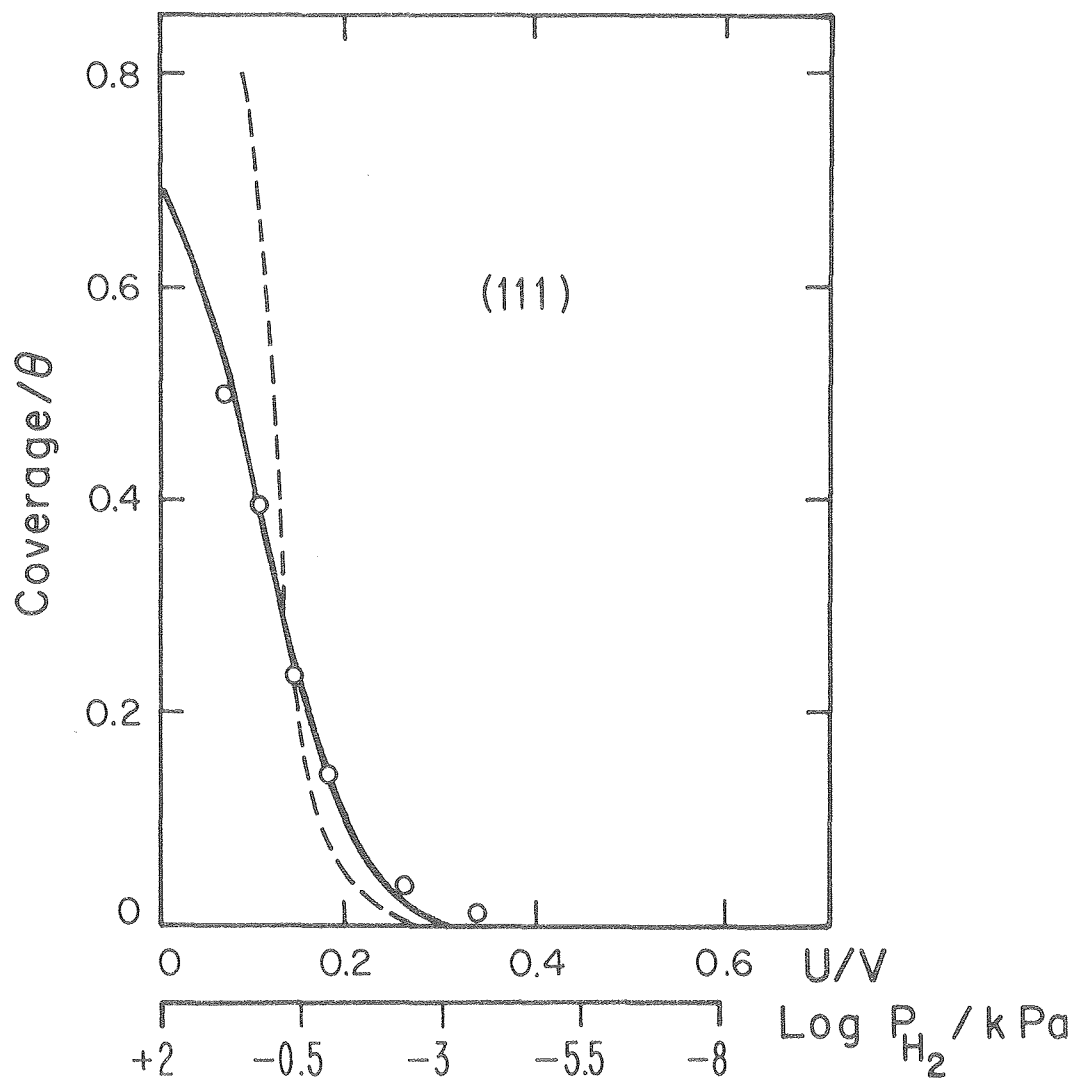Fig. 3

XBL 804-667

Fig. 4

Fig. 5

XBL 804-665

(111)
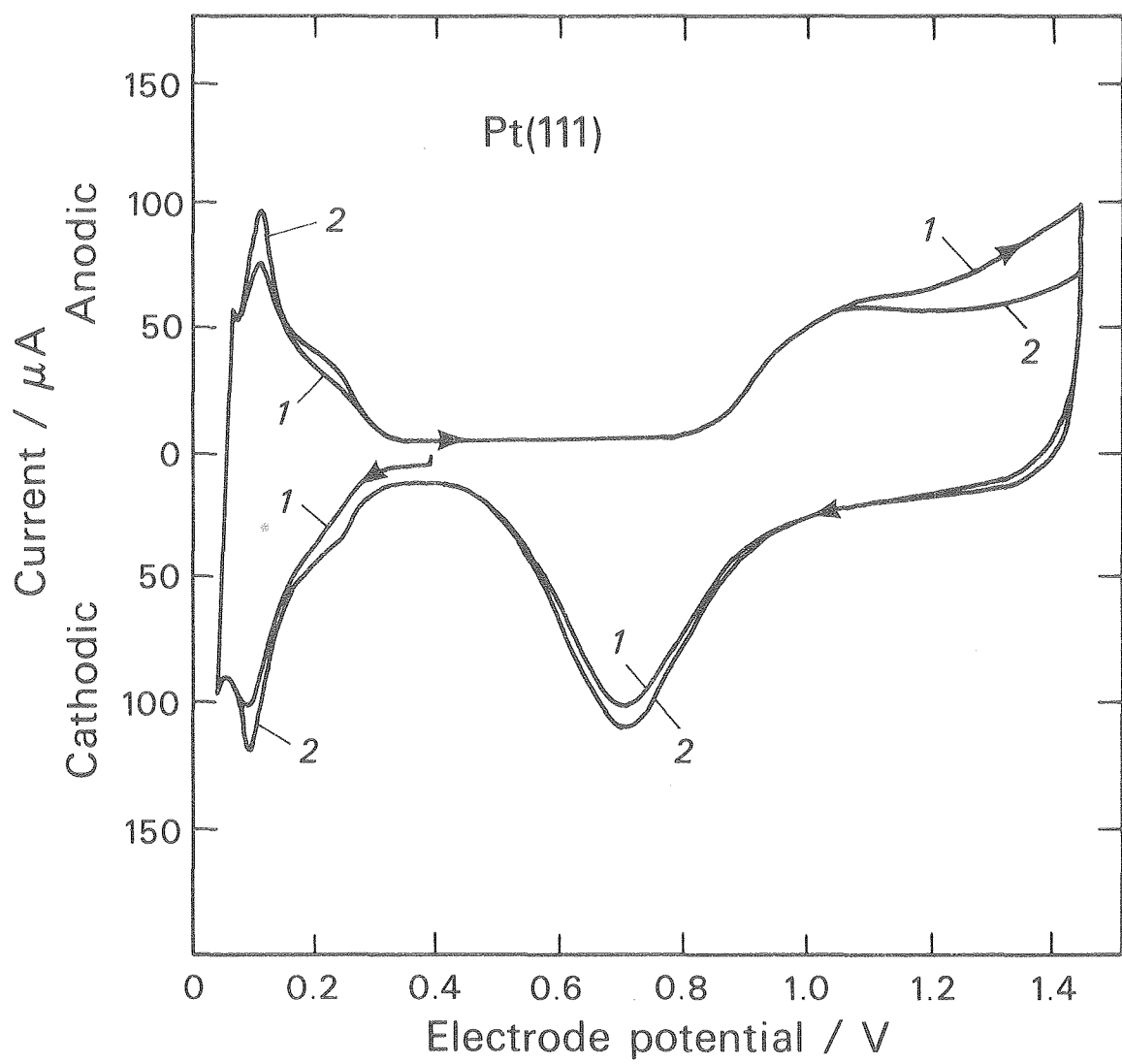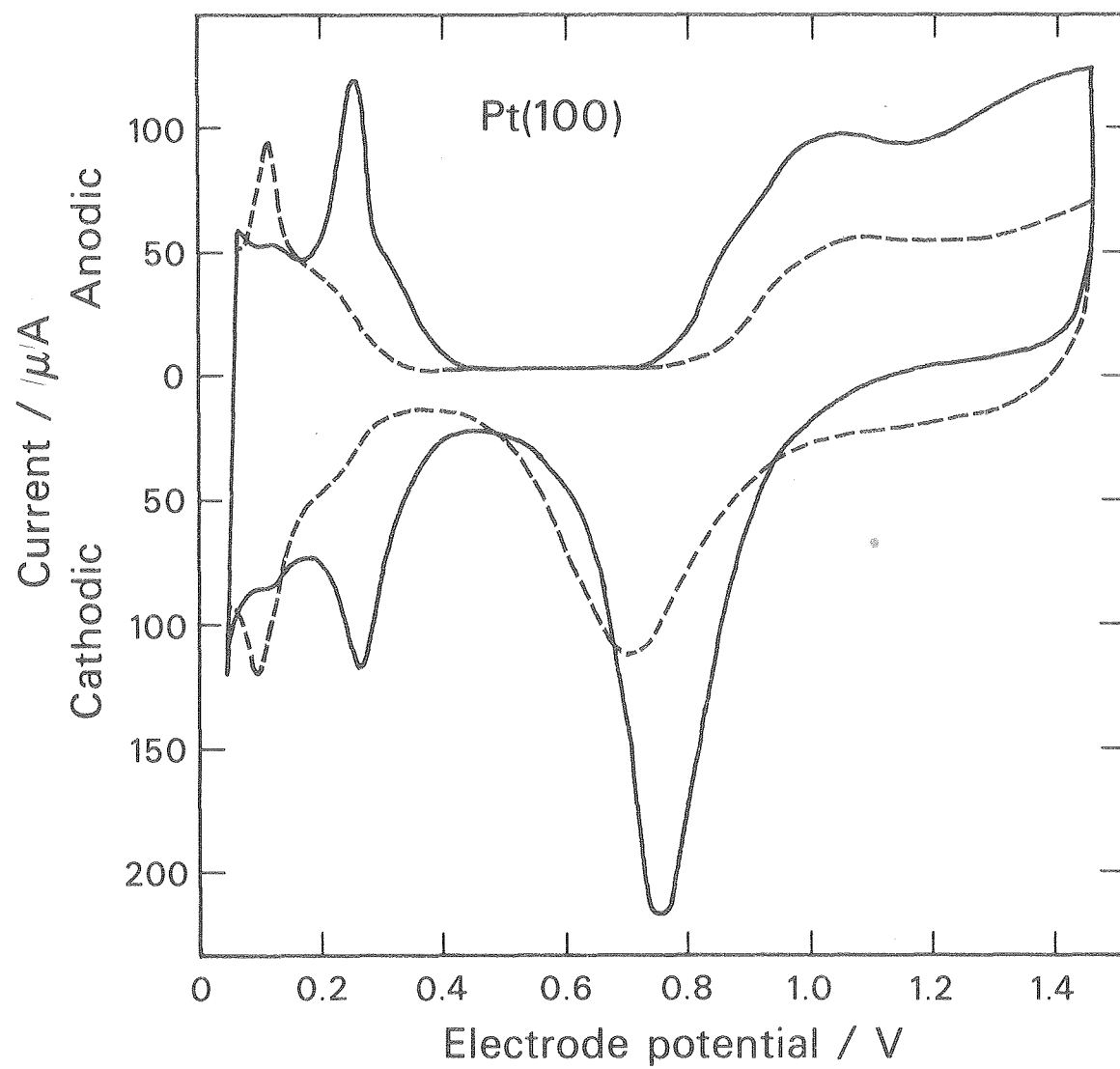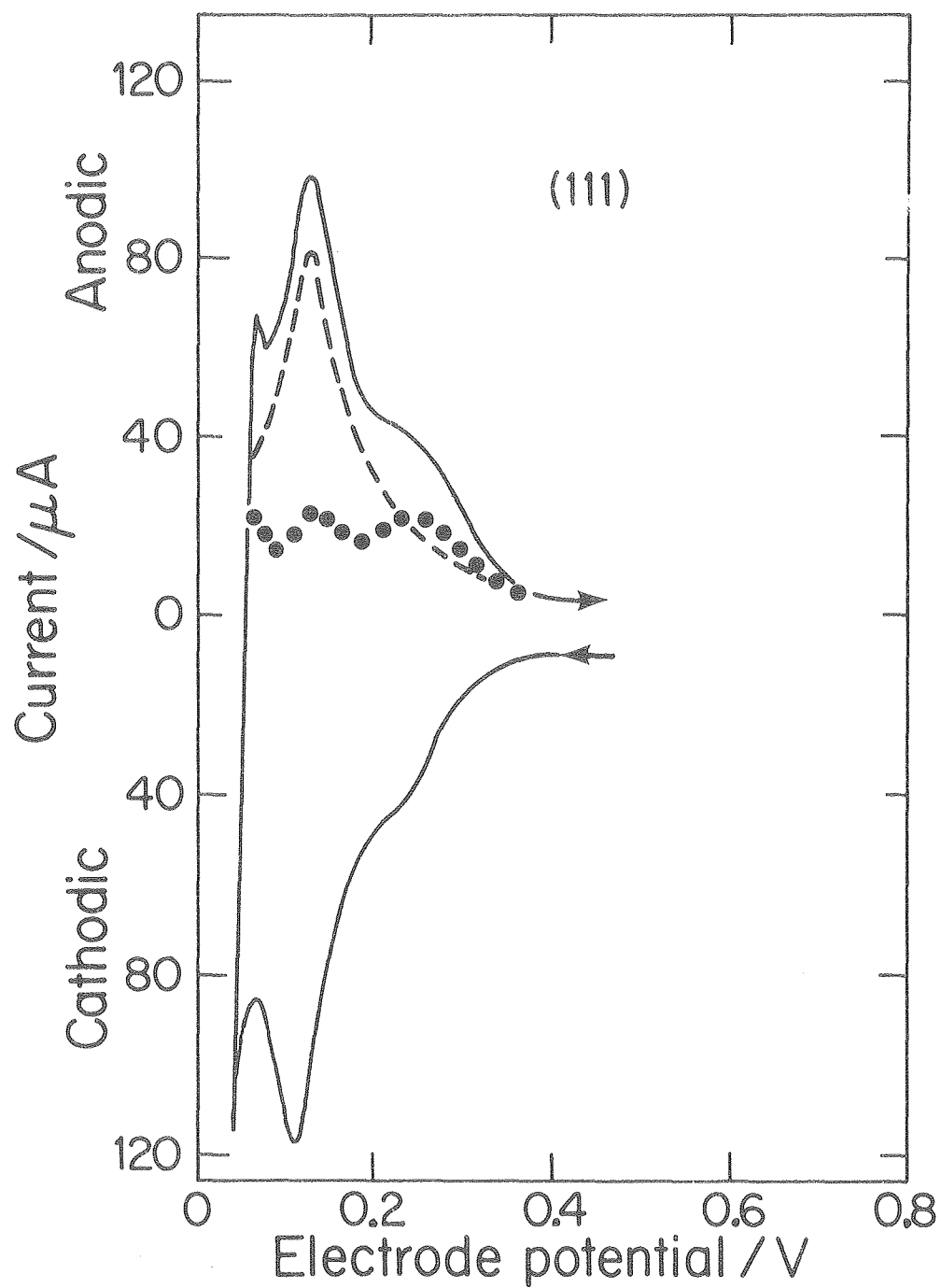
XBL 801 - 9

Fig. 6

Fig. 7
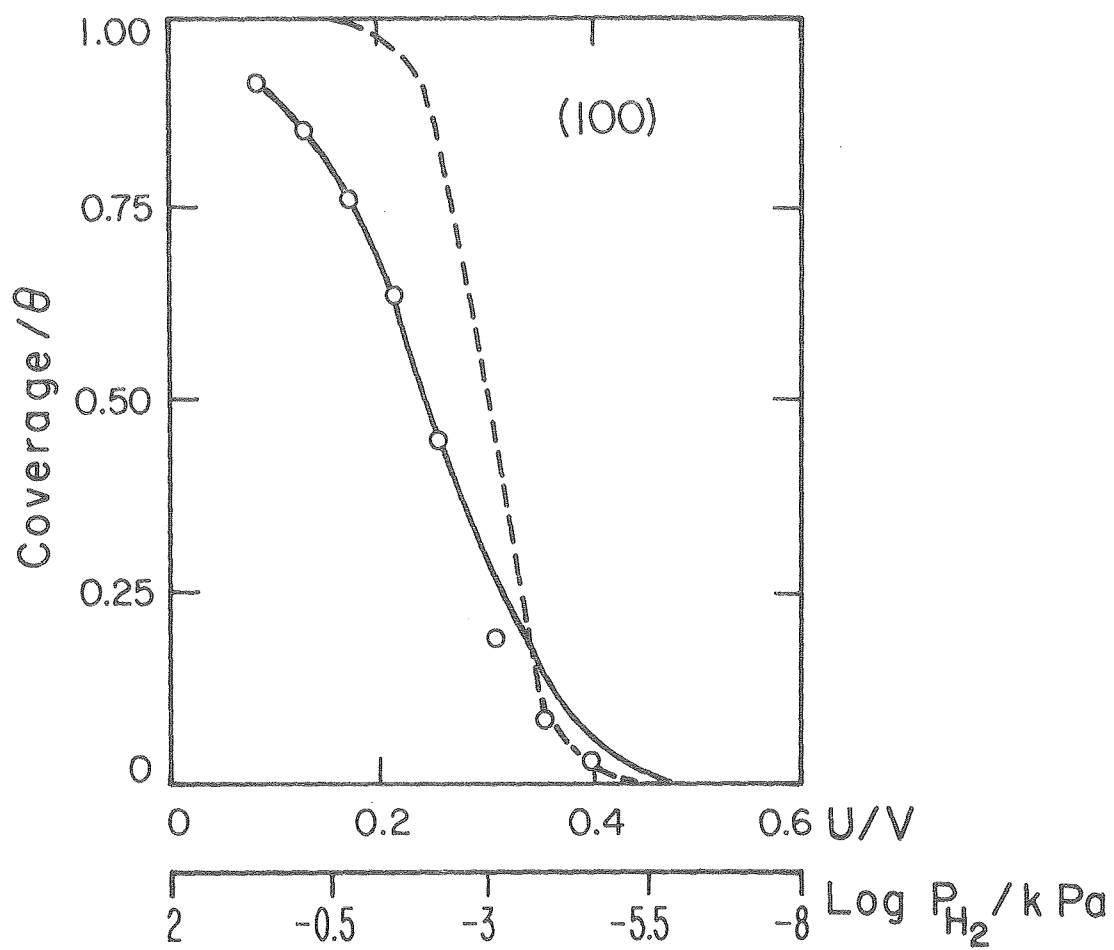
XBL 801-7

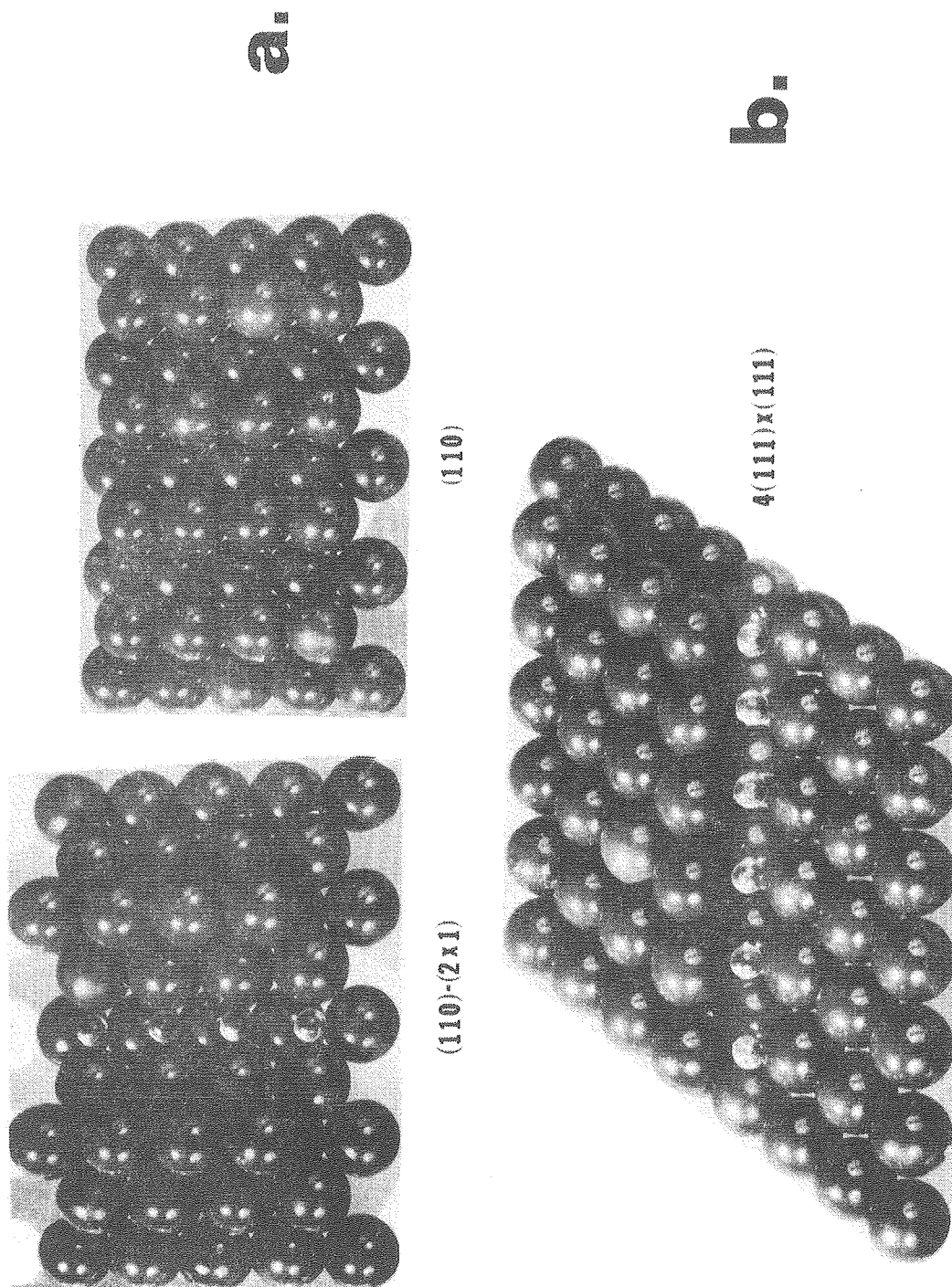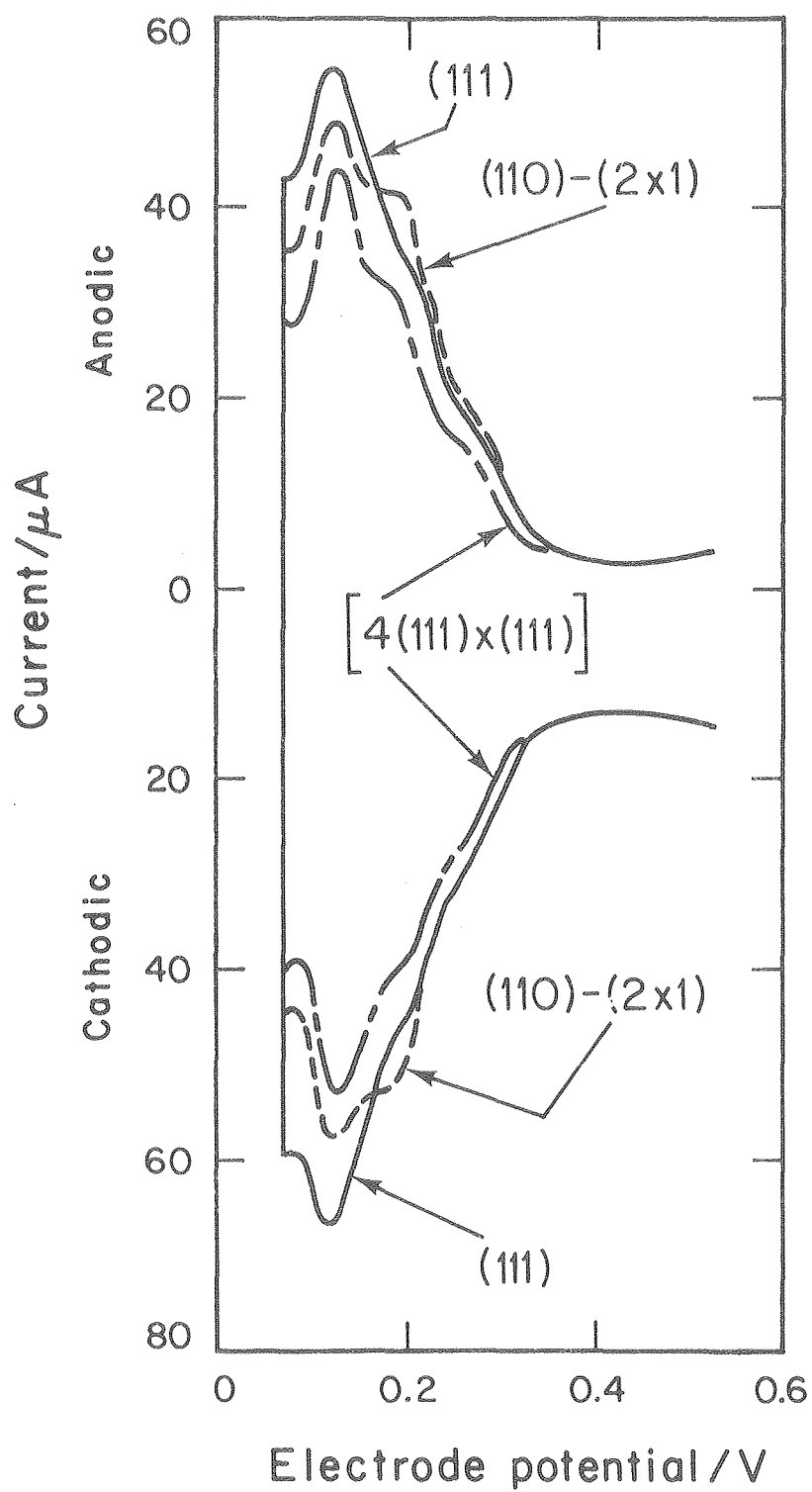XBL 802-195

Fig. 8

XBL802-196

Fig. 9

XBL802-199

Fig. 10

a.

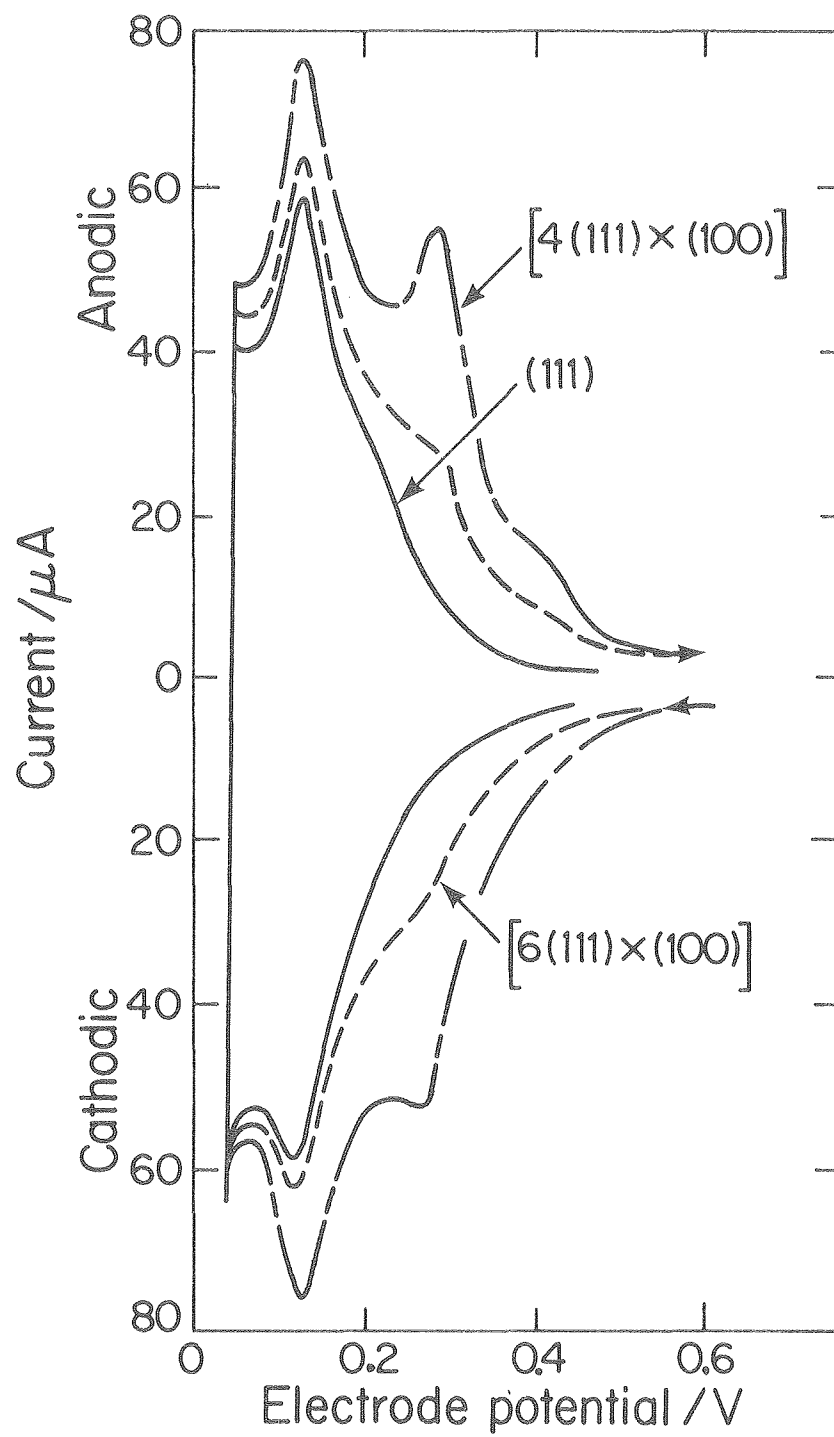(110)

(110)-(2 x 1)
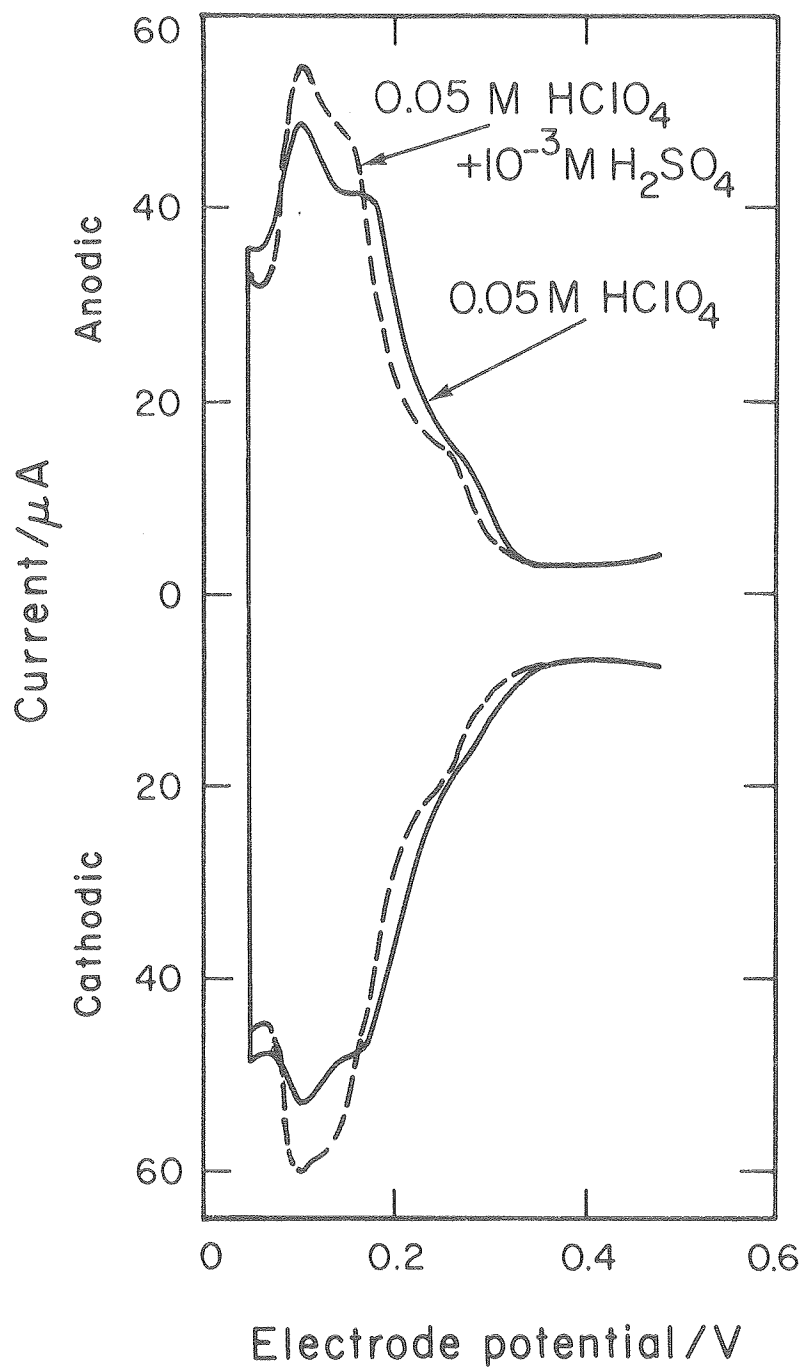
b.

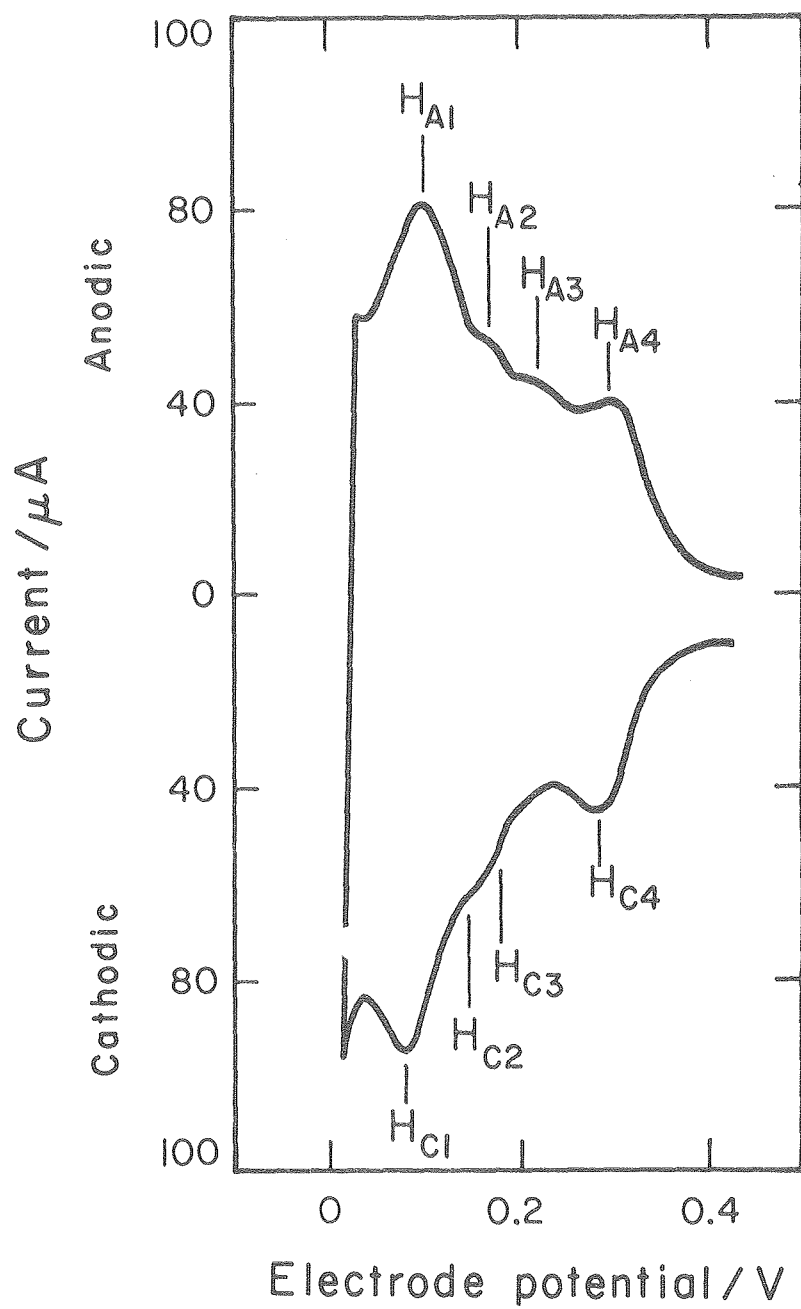4(111)x(111)

XBB 804-4104

Fig. 11

XBL 802-194

Fig. 12

Fig. 13

XBL 801 - 8

Fig. 14

XBL 802-197

XBL 802-198

Fig. 15